Indoleglycerol Phosphate Synthase−Phosphoribosyl Anthranilate Isomerase: Comparison of the Bifunctional Enzyme from *Escherichia coli* with Engineered Monofunctional Domains†

Marc Eberhard,‡ Monika Tsai-Pflugfelder,§ Krystyna Bolewska,|| Ulrich Hommel,⊥ and Kasper Kirschner*

Abteilung Biophysikalische Chemie, Biozentrum der Universität Basel, Klingelbergstrasse 70, CH-4056 Basel, Switzerland

Received August 5, 1994; Revised Manuscript Received November 7, 1994⊗

ABSTRACT: Putative domain−domain interactions of the monomeric bifunctional enzyme indoleglycerol phosphate synthase:phosphoribosyl anthranilate isomerase from *Escherichia coli* were probed by separating the domains on the gene level and expressing them as monofunctional proteins. The engineered monofunctional enzymes were found to be stable, monomeric proteins with virtually full catalytic activity. In addition, binding of indolylglycerol phosphate to the active site of indoleglycerol phosphate synthase and binding of reduced 1-[(2-carboxyphenyl)amino]-1-deoxyribulose 5-phosphate, a competitive inhibitor of both indoleglycerol phosphate synthase and phosphoribosyl anthranilate isomerase, were almost identical in both the mono- and bifunctional enzymes. Furthermore, no association between the monofunctional enzymes was found, neither *in vitro*, by sedimentation and gel filtration experiments, nor *in vivo*, by coexpression of the domains in the same cell. Thus, no selective advantages of the bifunctional enzyme from *Escherichia coli* over the respective monofunctional enzymes were found on a functional level. However, the phosphoribosyl anthranilate isomerase domain appears to stabilize the indoleglycerol phosphate synthase domain of the bifunctional enzyme from *Escherichia coli* by interactions that seem to subtly influence the kinetics of ligand binding.

Genes of biosynthetic pathways are found in a variety of arrangements, either as single genes or as part of operons, producing monofunctional single-domain proteins in some organisms and subunits of multienzyme complexes or multifunctional proteins in others. Some of the activities of the tryptophan biosynthesis pathway are known to be part of multifunctional enzymes (Crawford, 1989). A general tendency throughout evolution to condense different activities, in particular subsequent steps of metabolic pathways, into multifunctional proteins has been postulated (Hütter et al., 1986). By inference, multifunctional enzymes should have selective advantages over their monofunctional counterparts. Consecutive steps in a biosynthetic pathway may be catalyzed by two interacting active sites, such that the intermediate is confined to a channel between the active sites, as is found in tryptophan synthase (Hyde et al., 1988). As a further characteristic of this enzyme, the interaction between the α- and β-subunits provides for cooperative and allosteric regulation of enzymatic activity (Kirschner et al., 1991; Lane & Kirschner, 1991; Brzovic et al., 1992). Multidomain proteins might fold more rapidly or may be thermodynamically more stable than the respective single-domain enzymes.

The enzyme PRAI,[1] which catalyzes the Amadori rearrangement of PRA to CdRP (Scheme 1; Kirschner et al., 1987), is a monomer in yeast (Braus et al., 1988), but is part of a bifunctional, monomeric protein in *Escherichia coli*, termed IGPS:PRAI. The N-terminal part catalyzes the IGPS reaction, while the C-terminal domain is responsible for the PRAI reaction, the preceding step in the biosynthesis of tryptophan (Scheme 1; Creighton, 1970; Kirschner et al. 1980). The crystal structure of the bifunctional IGPS:PRAI revealed the presence of two nonoverlapping active sites, each formed by a $(\beta\alpha)_8$-barrel domain (Priestle et al., 1987; Wilmanns et al., 1992). Therefore, substrate channeling is ruled out. Moreover, kinetic studies (Cohn et al., 1979; Bisswanger et al., 1979) failed to reveal any interactions between the sites. Nevertheless, an interaction between the active sites may occur indirectly through the domain−domain interface (Wilmanns et al., 1992). This type of interaction may slightly alter the active site geometry of both enzymes and therefore alter their catalytic properties.

One strategy to analyze the effect of domain−domain interactions is to separate the domains and to isolate them as monofunctional enzymes (Steward et al., 1990; Hum & MacKenzie, 1991). Before the crystal structure of IGPS:

† This work was supported by Grant 3.255-1.85 from the Swiss National Science Foundation.

* Author to whom correspondence should be addressed.

‡ Present address: Department of Research, Cantonal Hospital, CH-4031 Basel, Switzerland.

§ Present address: ISREC, Chemin des Boveresses 155, CH-1066 Epalinges, Switzerland.

|| Present address: Institute of Biochemistry and Biophysics, Polish Academy of Sciences, ul. Rakowiecka 36, 02-532 Warszawa, Poland.

⊥ Present address: Sandoz Pharma AG, Lichtstrasse 35, CH-4002 Basel, Switzerland.

⊗ Abstract published in *Advance ACS Abstracts,* March 15, 1995.

[1] Abbreviations: PRA, *N*-(5′-phosphoribosyl)anthranilate; CdRP, 1-[(2-carboxyphenyl)amino]-1-deoxy-D-ribulose 5-phosphate; rCdRP, reduced CdRP; IGP, indoleglycerol phosphate; PRPP, 5′-phosphoribosyl 1-diphosphate; PRT, *N*-(5′-phosphoribosyl)anthranilate phosphoribosyl transferase (EC 2.4.2.18); PRAI, PRA isomerase or *N*-(5-phospho-β-D-ribosyl)anthranilate ketol-isomerase (EC 5.3.1.24); IGPS, IGP synthase or 1-[(2-carboxyphenyl)amino)-1-deoxy-D-ribulose-5-phosphate carboxylase (cycling) (EC 4.1.1.48); SDS, sodium dodecyl sulfate; EDTA, ethylenedi(nitrilo-*N*,*N*,*N*′,*N*′-tetraacetic acid; GuCl, guanidinium chloride; DTE, 1,4-dithioerythritol; FPLC, fast protein liquid chromatography; HPLC, high-performance liquid chromatography; rpm, rotations per minute.

0006-2960/95/0434-5419$09.00/0

Scheme 1

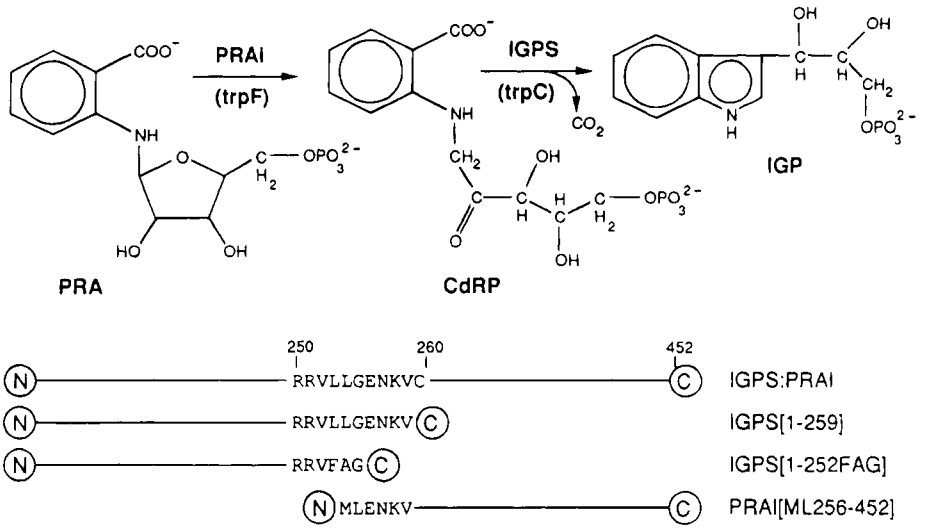

PRAI was elucidated it had been shown by limited proteolysis (Kirschner et al., 1980) that the large amino-terminal tryptic fragment of IGPS:PRAI, which comprises residues 1−289, catalyzes the IGPS reaction, whereas the overlapping carboxyl-terminal V8 fragment (residues 158−452) catalyzes the PRAI reaction. These results show that the corresponding domains can refold independently into their active structure. The crystal structure of IGPS:PRAI (Priestle et al., 1987) identified Gly 255 as the transition residue between the two $(\beta\alpha)_8$-barrel domains. With this information, it was feasible to produce the two monofunctional enzymes as $(\beta\alpha)_8$-barrel with non-overlapping amino acid sequences by genetic engineering. In the present study, we have constructed a truncated gene expressing a monofunctional IGPS comprising residues 1−259 of IGPS:PRAI (IGPS[1−259], Scheme 1) and a bicistronic operon for the simultaneous expression of the two domains (IGPS[1−252FAG] and PRAI[ML256−452]; Scheme 1), while considering whether the two surgically separated proteins form a stable noncovalent complex. We show that the separated IGPS and PRAI domains do not form a noncovalent bienzyme complex, but that they have very similar catalytic and ligand binding properties by comparison to the bifunctional enzyme. The IGPS domain appears to be stabilized by interaction with the covalently associated PRAI domain.

EXPERIMENTAL PROCEDURES

Buffers

Buffer A: 0.05 M Tris-HCl, (pH 7.5). Buffer B: 0.1 M Tris-HCl, (pH 7.8) containing 5 mM EDTA and 2 mM DTE. Buffer C: 0.05 M Tris-HCl, pH 7.5, containing 4 mM K_2-MgEDTA and 2 mM DTE.

Substrates and Inhibitors

PRA was synthesized enzymatically (Hommel et al., 1989) as follows: 10 μM anthranilic acid and 120 μM PRPP were dissolved in buffer C and converted to PRA by the addition of 0.2 munit of yeast PRT. One unit of activity is defined as the amount of enzyme that catalyzes the conversion of 1 μmol of substrate to products per minute at 25 °C under assay conditions. CdRP was synthesized in the same way by the further addition of 2 munits of xPRAI (Luger et al., 1989, 1990) or PRAI[ML256−452] (cf. Scheme 1 for enzyme terminology). No attempt was made to remove excess $MgCl_2$ and PRPP, as independent controls showed that these compounds did not influence any of the experiments described. The final concentration of CdRP was adjusted by appropriate dilution of the preparation. IGP was obtained by the conversion of 10 μM CdRP with 2 munits of IGPS:PRAI. The enzymes present in the preparations (PRT, PRAI, or IGPS) were removed by ultrafiltration (Centricon TM-10) whenever they would interfere with the subsequent experiment. rCdRP was synthesized by the reduction of CdRP according to Bisswanger et al. (1979). Chemically synthesized substrates (Kirschner et al., 1987) were used for following the active enzyme during protein purification. The concentrations of substrates and rCdRP were determined as described elsewhere (Hommel et al., 1995).

Plasmids

Transformation of *E. coli* and all DNA manipulations were performed according to standard procedures (Maniatis et al., 1982). M13mp9trpC(F), pUC8trpC(F), and pMa114trpC-(F) (cf. Table 1 for terminology) were obtained by inserting the *Hin*dIII fragment of pWS1 (Schneider et al., 1981) bearing the *trpC(F)* gene of *E. coli* into the *Hin*dIII site of M13mp9 (Messing & Vieira, 1982), pUC8 (Vieira and Messing, 1982), and pMa114 (Stanssens et al., 1989), respectively.

Construction of M13mp9trpCF (Bicistronic Operon; Eberhard (1990a) p 37). In a first step, two unique restriction sites (*Asu*II and *Xho*I) were introduced into M13mp9trpC-(F) at the connector between the two domains, i.e., Gly 255 (Priestle et al., 1987), by means of site-directed mutagenesis (Kramer et al., 1984). The oligonucleotide used, (5′-GCCGGGTGTTCGAACTCGAGAATAAGTAT-3′, mismatches underlined), also changes Leu 253 to Phe and Ala to Leu 254 [amino acid numbering according to Priestle et al., (1987)]. The resulting construct was cut with the restriction enzymes *Asu*II and *Xho*I and ligated with a fragment of synthetic, double-stranded DNA containing a stop codon and a designed ribosomal binding site (Shine & Dalgarno, 1974). Samples of 100 pmol of each of the oligonucleotides (5′-CGCGGGTTAAGGAGGTACCTATAT-

GC-3′ and 3′-GCCCAATTCCTCCATGGATATACGAGCT-5′) were combined, annealed, and 5′-phosphorylated according to standard procedures (Maniatis et al., 1982). The correct sequence of the resulting construct (M13mp9trpCF, Table 1) was confirmed by DNA sequencing [M13 cloning and sequencing handbook, Amersham International Plc., (1983); method according to Sanger et al. (1977)].

Construction of pMc2CF. M13mp9trpCF was cut with *Hin*dIII and *Aos*I to yield a 1511 bp fragment. pMc510 (Stanssens at al., 1989) was linearized by cutting with *Cla*I, and the recessed 3′-ends were filled up by means of DNA polymerase I (Klenow fragment) and subsequently cut with *Hin*dIII. The resulting fragment (4059 bp in length) was ligated with the preceding 1511 bp fragment to yield pMc2CF.

Other Vectors. pMc2C was constructed in the same way as pMc2CF by using pWS1′ instead of M13mp9trpCF. pWS1′ is a variant of pWS1 containing an engineered Cys 260 to amber mutation in the *trpC(F)* gene (Pflugfelder, 1986). DNA sequencing of pMc2CF [Sequenase manual, United States Biochemical; method according to Sanger et al. (1977)] revealed an A to G mutation in the trpF region, changing Val 330 to Ala. Otherwise, no deviation from the published nucleotide sequence (Horowitz et al., 1983) was found. pUC8CF and pWS1CF were constructed by replacing the *Hin*dIII fragments of pUC8trpC(F) and pWS1, respectively, with that of M13mp9trpCF.

Protein Purification

xPRAI, a recombinant version of yeast PRAI expressed in *E. coli*, was purified according to Luger et al. (1989, 1990); yeast PRT was purified according to Hommel et al. (1989). IGPS:PRAI from *E. coli* was prepared as described (Kirschner et al., 1987).

PRAI[ML256−452]. All steps were performed at 0 or 4 °C. Buffers were supplemented with 2 mM EDTA and 1 mM DTE. *E. coli* cells W3310 *trp*R, Δ*trp*EA2 (Schneider et al., 1981) were transformed with pMc2CF (Table 1) and grown in 35 L of Luria−Bertani medium (Maniatis et al., 1982) supplemented with 30 μg chloramphenicol/mL in a 50 L fermentor (Bioengineering). Cells (typically 190 g of wet weight) were harvested after 10 h of growth (apparent absorbance at 550 nm around 5.4), washed with 0.05 M potassium phosphate buffer (pH 7.0), frozen at −20 °C, thawed, and resuspended in 600 mL of 0.01 M potassium phosphate buffer (pH 7.5) containing 0.1 mM phenylmethanesulfonyl fluoride. The cell suspension was sonicated three times for 40 s (Branson B-12 cell disruptor), taking care to keep the suspension cool. The extract was centrifuged (5000 rpm for 30 min, Sorvall GS-3 rotor), and the pellet was saved for the purification of IGPS[1−252FAG] (cf. below). Protamine sulfate (2.5 g) dissolved in 50 mL of 0.01 M potassium phosphate buffer (pH 7.5) was added dropwise to the supernatant to precipitate DNA, and the suspension was clarified by two successive centrifugations (12 000 rpm for 30 min, Sorvall GS-3 rotor). The clear supernatant was pumped onto a column (5 x 41.5 cm) of DEAE-Sepharose fast flow that had been equilibrated previously with 0.01 M potassium phosphate buffer (pH 7.5). After they were washed with 500 mL of the same buffer, proteins were eluted with a linear gradient of increasing concentration (10−300 mM) of potassium phosphate buffer (pH 7.5). PRAI activity appeared at approximately 140 mM potassium phosphate. Active fractions were pooled, concentrated by ultrafiltration (Amicon PM-10 membrane) to a volume of approximately 5 mL and a protein concentration of about 40 mg/mL, supplemented with 1 mL of 87% glycerol, clarified by centrifugation, and applied to a column (2.4 × 88 cm) of Sephadex G-75 previously equilibrated with 0.05 M potassium phosphate buffer (pH 7.0). Proteins were eluted isocratically with the same buffer. Active fractions were combined, adjusted to 15% glycerol, dripped into liquid nitrogen, and stored frozen at −70 °C.

IGPS[1−252FAG]. The pellet (10 g) containing inclusion bodies (cf. previous section) was washed with 0.05 M potassium phosphate buffer (pH 7.0) and resuspended in 20 mL of 0.01 M potassium phosphate buffer (pH 7.0) containing 100 mM KCl and 6 M GuCl. The solubilized material was clarified by two successive centrifugations (18 000 rpm, Sorvall SS-34 rotor) and applied to a column (5 × 83.5 cm) of Sephacryl S-200 previously equilibrated with 0.01 mM potassium phosphate buffer (pH 7.0) containing 0.1 M KCl and 2.5 M GuCl. Proteins were eluted isocratically with the same buffer. IGPS activity was measured after 50-fold dilution with buffer C. Active fractions were pooled, diluted with buffer C containing 3 M GuCl, and renatured by dialysis against buffer C containing 10% glycerol.

IGPS[1−259]. Crude cell extract was prepared from *E. coli* W3110 *trp*R, Δ*trp*EA2 transformed with pMc2C (Table 1), as described under the paragraph on PRAI[ML256−452]. The crude extract was pumped onto a column (5 × 41.5 cm) of DEAE-Sepharose fast flow previously equilibrated with 0.02 M potassium phosphate buffer (pH 7.0). The column was washed with the same buffer and subsequently eluted with a linear gradient (20−500 mM) of potassium phosphate buffer (pH 7.0). IGPS activity appeared at approximately 230 mM potassium phosphate. Active fractions were pooled and concentrated to about 30 mg/mL by ultrafiltration (Amicon PM-10 membrane). Eight milliliters of the concentrate was supplemented with 1.5 mL of 87% glycerol, clarified by centrifugation, and applied to a column (4 × 92 cm) of Sephadex G-75 equilibrated with 0.05 M potassium phosphate buffer (pH 7.0). Proteins were eluted isocratically using the same buffer. Active fractions were pooled, dripped into liquid nitrogen after the addition of 15% glycerol, and stored frozen at −70 °C.

Determination of Protein Concentration

Protein concentrations were determined spectrophotometrically using the following extinction coefficients: IGPS:PRAI, $\epsilon_{278} = 0.84$ cm^2 mg^{-1} (Kirschner et al., 1987); IGPS[1−259], $\epsilon_{280} = 0.81$ cm^2 mg^{-1}; PRAI[ML256−452], $\epsilon_{280} = 1.10$ cm^2 mg^{-1}; xPRAI, $\epsilon_{280} = 1.3$ cm^2 mg^{-1}. The extinction coefficients of IGPS[1−259] and PRAI[ML256−452] were determined by amino acid analysis, after 24 h of hydrolysis with 6 M HCl at 110 °C followed by dabsylation and quantitative analysis by HPLC using a 5 μm C-18 column from Merck, according to Knecht and Chang (1986). The extinction coefficient of xPRAI was determined by second-derivative spectroscopy according to Levine and Federici (1982). During purification, protein concentrations were estimated using the Bio-Rad protein assay (Bradford, 1976) with IGPS:PRAI as standard.

Table 1: Plasmids Used for the Expression of trpC and trpF Genes

plasmid	gene	gene product
M13mp9trpC(F)[a]	*trpC(F)*	none[a]
pUC8trpC(F)	*trpC(F)*	IGPS:PRAI
pMa114trpC(F)[b]	*trpC(F)*	IGPS:PRAI
M13mp9trpCF[a]	*trpCF*[c]	none[a]
pUC8CF	*trpCF*[c]	IGPS[1−252FAG], PRAI[ML256−452]
pWS1CF	*trpCF*[c]	IGPS[1−252FAG], PRAI[ML256−452]
pMc2CF	*trpCF*[c]	IGPS[1−252FAG], PRAI[ML256−452]
pWS1′[d]	*trpC*	IGPS[1−259]
pMc2C	*trpC*	IGPS[1−259]

[a] The indicated genes of these constructs are present in the reverse orientation with respect to the promoter and therefore are not expressed. *trpC(F)* represents the gene encoding the wild-type bifunctional IGPS:PRAI. [b] Hommel (1988). [c] Bicistronic operon. [d] Pfugfelder (1986).

Determination of Molecular Weights

Sedimentation experiments were performed with a Beckman Model E ultracentrifuge equipped with ultraviolet optics and a photoelectric scanner. Sedimentation velocity experiments were carried out at 21 °C and 52 000 rpm using an An-D rotor with 12 mm DS-Epon cells. Molecular weights were determined from equilibrium sedimentation (18 °C, 20 000 rpm) using a linear least-squares fit of the logarithm of A_{280} versus the squared distance from the rotor center. Sedimentation coefficients were calculated from the midpoint of the moving boundary (Schlieren optics for protein concentrations higher than 5 mg/ml; UV absorbance for concentrations around or below 1 mg/mL). Analytical gel filtration was carried out by FPLC using a column of Superose 12 (1 × 30 cm, 23 mL volume, Pharmacia). Experiments were conducted in 0.05 M potassium phosphate buffer (pH 7.0) containing 200 mM KCl, 5 mM EDTA, and 2 mM DTE at room temperature. The column was calibrated with cytochrome *c* (horse heart, M_r = 12 400), bovine myoglobin (17 000), bovine carbonic anhydrase (30 000), bovine serum albumin (66 300), and phosphorylase *b* (rabbit muscle, 194 800) and gave a linear relationship between the logarithm of M_r and the elution volume.

Small Scale Expression Assays

Luria−Bertani medium (5 mL)containing the appropriate antibiotic (Maniatis et al., 1982) were inoculated with a single colony of the strain to be assayed. Cells were grown overnight at 37 °C, and 1 mL of culture was pelleted and resuspended in 400 μl of buffer C. Cells were homogenized by sonication (3 × 20 s at 0 °C, with pauses to allow for the dissipation of heat). The homogenate was centrifuged and the supernatant assayed for enzyme activity. The pellet was extracted with buffer C containing 3 M GuCl and assayed after 50-fold dilution at 0 °C with buffer C, followed by a refolding period of 30 min.

Enzyme Assays

Both enzyme assays and progress curve evaluation were performed as described elsewhere (Hommel et al., 1995). It was observed that the fluorescence of IGP (excitation at 280 nm, emission at 350 nm) decreased upon prolonged exposure to the excitation light. Therefore, the progress time of the IGPS reaction was kept below 3 min by adjusting the enzyme concentration. During protein purification and for testing expression levels, both PRAI and IGPS activity was measured according to Kirschner et al. (1987).

Ligand Binding

Fluorescence spectra were recorded with an SLM series 8000 instrument interfaced to an HP 9815A computer. Solutions of ligand were added with AGLA micropipets. Titrations were analyzed with the most simple model involving the binding of L (ligand) to a single site on P (protein) to form a complex denoted PL (eq 2). The degree of saturation, defined as $x = [\overline{PL}]/[P]_o$, where $[\overline{PL}]$ is the equilibrium concentration of PL and $[P]_o$ is the total concentration of protein, was obtained by

$$x = \frac{1}{2\sqrt{b^2 - 4c}} \qquad (1)$$

where

$$b = 1 + ([L]_o + K_d)/n[P]_o \qquad c = [L]_o/n[P]_o$$

$[L]_o$ is the total ligand concentration, K_d represents the thermodynamic dissociation constant, and n is the effective number of binding sites per protein molecule. The kinetics of ligand binding was measured by stopped-flow experiments with the Durrum equipment described by Paul et al. (1980). Experimental data were analyzed by means of nonlinear least-squares fitting (Marquardt, 1963; Eberhard, 1990b).

RESULTS

Expression of the Monofunctional Enzymes. Efficient expression of the monofunctional enzymes was achieved by placing the genes under control of the λp_L promoter of pMc2, a modified pMa/c vector (Stanssens et al., 1989; cf. Experimental Procedures). The modified vectors (Table 1) were designed to have a shorter distance between promoter and the first ATG codon (177 versus 651 base pairs) than in the original construct pMa114trpC(F) (cf. Experimental Procedures). For the simultaneous expression of the PRAI and IGPS domain, a bicistronic operon was constructed by inserting a linker containing a stop codon, a ribosomal binding site, and a start codon into the gene encoding IGPS:PRAI. Due to the new restriction sites required for inserting the synthetic intercistronic region, both domains contain minor changes with respect to the original sequence (IGPS[1−252FAG], PRAI[ML256−452]; cf. Scheme 1). Whereas the gene encoding IGPS[1−252FAG] uses its endogenous ribosomal binding site, the gene for PRAI[ML256−452] contains a synthetic consensus sequence of the ribosomal binding site. The *E. coli* strain used for expression (W3110 *trp*R, Δ*trp* EA2) lacks the entire *trp* operon, thus precluding contamination by wild-type IGPS:PRAI.

The yields of IGPS[1−259], IGPS[1−252FAG], and PRAI[ML256−452] obtained by expressing the corresponding pMc2 vectors in *E. coli* W3110 *trp*R, Δ*trp* EA2 proved to be far superior to those obtained with the other vectors listed in Table 1. IGPS was found in both inclusion bodies and soluble extracts of transformants carrying pMc2C (cf. Experimental Procedures under Small Scale Expression Assay). In soluble extracts of pMc2C transformants, IGPS[1−259] accumulates to approximately 30% of total protein

as judged from polyacrylamide gel electrophoresis in the presence of SDS. The soluble fraction of transformants carrying pMc2CF contained PRAI but no IGPS activity, whereas the insoluble fraction contained both PRAI and IGPS. In soluble cell extracts, PRAI[ML256−452] accumulates to approximately 5% of total protein, whereas IGPS[1−252FAG] accounts for approximately 30% of total protein in inclusion bodies. No soluble IGPS activity was found when the bicistronic operon was placed into vectors that expressed the genes at different levels (pUC8CF < pWS1CF < pMc2CF, cf. Table 1; data not shown) or when the bicistronic operon was expressed transiently, using the K12 strain of *E. coli* that produces a thermolabile λcI repressor and the pMc2CF vector (Stanssens et al., 1989).

Purification of the Monofunctional Enzymes. IGPS[1−252FAG] was readily renatured either from GuCl extracts of the insoluble fraction or after gel filtration chromatography of the GuCl extract in the presence of 2.5 M GuCl, by 50-fold dilution with ice-cold Tris-HCl buffer. At final protein concentrations below 0.5 μM (0.014 mg/mL) the renaturation yields were at least 90%. Renaturation with about the same efficiency was also achieved by dialysis. However, renatured IGPS[1−252FAG] was found to precipitate when concentrated above 1 μM (29 μg/mL). Moreover, the nature of the buffer, the temperature, the presence of reducing agents, and the pH value were found to be important for efficient renaturation. Tris-HCl buffer (0.05 M) at pH 8.0−8.5, 0 °C, and the presence of 1 mM DTE was found to be optimal. Various additives have been tested to increase the solubility of IGPS[1−252FAG], albeit unsuccessfully. While salts classified as cosmotropic in the Hoffmeister series (Washabaugh & Collins, 1986) had little effect at concentrations between 0.05 and 1 M, chaotropic salts increased the tendency of aggregation. Organic solvents (ethanol, methanol, acetone, and acetonitrile, each at 10%) caused precipitation. Inclusion of detergents in the buffer (1 mg/mL dodecyl β-D-maltoside, Triton X-100, and 3-(*N*-tetradecyl-*N*,*N*-dimethylammonio)-1-propanesulfonate; cf. Tandon & Horowitz, 1988) either decreased both the renaturation yield and the solubility or had no effect. Addition of 10% glycerol to the buffers increased the renaturation yield slightly. As a consequence of the tendency to form aggregates, purification of native IGPS[1−252FAG] resulted in precipitation on chromatography columns.

Both IGPS[1−259] and PRAI[ML256−452] were found in soluble extracts of cells expressing the respective gene (cf. Table 1). In order to avoid tedious renaturation procedures, both IGPS[1−259] and PRAI[ML256−452] were purified from soluble cell extracts (Table 2). Neither IGPS[1−259] nor PRAI[ML256−452] aggregated upon ultrafiltration to a protein concentration of 10 mg/mL in 0.05 M potassium phosphate buffer (pH 7.0). In contrast, IGPS[1−259] aggregates at concentrations above 0.3 mg/mL in Tris-HCl buffer (concentration between 0.01 and 0.1 M, pH 8.0). The choice of buffer is also critical for the optimal resolution of IGPS[1−259] on DEAE-Sepharose columns. In Tris buffer, the protein elutes as a broad peak with a gradient of NaCl, and a large fraction precipitates on the column, at both pH 7.5 and 8.2. In contrast, a gradient of phosphate buffer at pH 7.0 elutes IGPS[1−259] as a sharp peak with high yield.

Hydrodynamic Properties. We used gel filtration on Superose 12 columns under native conditions to assess the tendency of the separated domains to aggregate. For example, IGPS[1−259] cystallizes as a trimer from phosphate buffer (pH 5.0) containing ammonium sulfate (Wilmanns et al., 1990). Moreover, we wanted to check whether the separated domains are still capable of forming a stoichiometric noncovalent complex. Earlier studies involving sucrose gradient centrifugation of an equimolar mixture of IGPS[1−259] and an extended, genetically engineered PRAI domain (Pflugfelder, 1986) had failed to demonstrate such a complex, but the overlap of the respective carboxyl- and amino-terminal extensions of these domains might sterically hinder complementary noncovalent interactions.

As shown by gel filtration, IGPS[1−252FAG], IGPS[1−259], and PRAI[ML256−452] eluted at the monomer position (Table 3). Moreover, IGPS[1−259] remained monomeric in the pH range between 5.0 and 7.0, although this protein has a higher tendency to aggregate upon prolonged incubation than has PRAI[ML256−452]. Sedimentation experiments were carried out to confirm the preceding results (Table 4). Unfortunately, because of its limited solubility (less than 0.02 mg/mL), IGPS[1−252FAG] could not be analyzed by this method. The results of the sedimentation experiments show that both PRAI[ML256−452] and IGPS[1−259] are monomeric in solution under all conditions examined.

Finally, no interaction between IGPS[1−252FAG] and PRAI[ML256−452] was found by gel the filtration of PRAI[ML256−452] in the presence of 0.18 μM IGPS[1−

Table 2: Purification of the Monofunctional Enzymes IGPS[1−252FAG], IGPS[1−259], and PRAI[ML256−452]

step	total activity (IU)	total protein (mg)	specific activity (IU/mg)	yield (%)
IGPS[1−252FAG][a]				
crude extract	160	157	1.0	100
Sephacryl S-200	126	60	2.1	79
IGPS[1−259][b]				
crude extract	458	6320	0.073	100
DEAE-Sepharose	393	383	1.03	86
Sephadex G-75	350	102	3.43	77
PRAI[ML256−452][c]				
crude extract	28360	10280	2.76	100
DEAE-Sepharose	13950	211	66.1	49
Sephadex G-75	10360	105	98.7	37

[a] Purification of IGPS[1−252FAG] from inclusion bodies of about 5 g of wet cells in the presence of 2.5 M GuCl. IGPS activity was measured after dilution with buffer C. [b] Purification from 166 g of wet cells. [c] Purification from 190 g of wet cells.

Table 3: Analytical Gel Filtration of Monofunctional IGPs and PRAI

protein	concentration[a] mg/mL)	elution volume (mL)	apparent M_r	expected M_r[b]
IGPS[1−252FAG]	0.0049	13.8	22 000	28 800
IGPS[1−259]	0.48	13.5	24 000	28 900
IGPS[1−259]	10.1	13.5−13.7[c]	23 000	28 900
PRAI[ML256−452]	0.25	13.6	23 000	21 200
PRAI[ML256−452] + IGPS[1−252FAG][d]	0.25	13.7	22 000	21 200

[a] Concentration of sample used for loading a column of Superose 12. See Experimental Procedures for details. [b] Calculated from the amino acid sequence, assuming monomeric proteins. [c] Range of elution volumes at 10 different pH values between 5.0 and 7.0. [d] In the presence of 0.18 μM (0.0052 mg/mL) IGPS[1−252FAG] in the equilibration and elution buffer.

Table 4: Analytical Ultracentrifugation of IGPS[1−259] and PRAI[ML256−452]

protein	concentration (mg/mL)	sedimentation coefficient	pH[a]
IGPS[1−259]	0.75	2.56 S	7.0
IGPS[1−259]	8.8	2.26 S	5.0
PRAI[ML256−452]	0.68	2.0 S	7.0
protein	concentration (mg/mL)	apparent molecular weight[b]	pH
IGPS[1−259]	0.25	31 500	7.0
PRAI[ML256−452]	0.3	23 000 (31 000)[c]	7.0

[a] 0.05 M potassium phosphate containing 2 mM EDTA and 1 mM DTE. [b] A partial specific volume of 0.73 $cm^3\ g^{-1}$ was assumed for both IGPS[1−259] and PRAI[ML256−452]. [c] Minor component.

252FAG] in the buffer (Table 3). Therefore, it is clear that the eight distinct hydrogen bonds that are found in the interdomain interface of the bifunctional enzyme (Wilmanns et al., 1992) do not suffice to stabilize a noncovalent complex between IGPS[1−252FAG] and PRAI[ML256−452].

Steady State Kinetics. With the availability of pure anthranilate phosphoribosyltransferase (PRT) and pure monofunctional PRAI[ML256−452], it was feasible to synthesize both PRA and CdRP enzymatically from PRA and PRPP.

$$\text{anthranilate} + \text{PRPP} \xrightarrow{\text{PRT}} \text{PRA} + \text{PP}_i \xrightarrow{\text{PRAI}} \text{CdRP} + \text{PP}_i$$

Spectroscopic analysis (Kirschner et al., 1987) of this preparation of CdRP by its quantitative conversion to IGP using monofunctional IGPS[1−259] revealed that the enzymatic conversion of anthranilic acid and PRPP to PRA and CdRP was essentially complete (cf. Hommel et al., 1995). Steady state kinetic constants determined either with chemically synthesized CdRP or with enzymatically produced CdRP were identical within experimental error, indicating that impurities present in the chemically synthesized substrate (e.g., ribose 5-phosphate, anthranilic acid) do not influence the enzyme assay of IGPS appreciably.

To avoid inhibition by the product CdRP, steady state kinetic constants were determined by analysis of the dependence of initial velocity on the substrate concentration (Cornish-Bowden, 1975; Figure 1). The product inhibition constant, K_P was determined separately by the evaluation of entire progress curves (Duggleby & Morrison, 1977; cf. Hommel et al., 1995; Figure 2). Progress curve analysis of IGPS[1−252FAG] was not possible, because the enzyme aggregated under assay conditions, and therefore no reliable data for possible product inhibition were obtained.

The progress curve of the PRAI reaction of wild-type IGPS:PRAI (data not shown) was measured in the presence of an excess of monofunctional IGPS[1−259] (final concentration 540 nM) to convert the inhibitory product CdRP to IGP and fitted to the integrated Michaelis−Menten equation that ignores product inhibition. Control experiments showed that PRAI is not inhibited by IGP up to a concentration of 2 μM.

Competitive inhibition constants of the substrate analogue rCdRP (Bisswanger et al., 1979) were determined for both IGPS[1−259] and PRAI[ML256−452] and were compared to those of the IGPS and PRAI domains of the wild-type bifunctional protein (Hommel et al., 1995). Inhibition of IGPS[1−252FAG] by rCdRP was not measurable due to problems with aggregation. The linear relationship between apparent K_M values and the concentration of the competitive inhibitor rCdRP (Figure 3) and the constant k_{cat} values at all inhibitor concentrations (not shown) are indicative of competitive inhibition. The pertinent data are collected in Table 5.

Ligand Binding. The binding of rCdRP caused a decrease in tryptophan fluorescence (excitation at 280 nm, emission at 340 nm) for each of the proteins studied. Moreover, the fluorescence of bound rCdRP (excitation at 330 nm, emission at 430 nm) can also be excited at 280 nm, because fluorescence energy is transferred from the tryptophan residues of the protein to rCdRP (Cohn et al., 1979). Thus, fluorescence excited at 280 nm and observable at 430 nm is a unique property of the protein−rCdRP complexes.

In the present study, both fluorescence quenching and fluorescence energy transfer were used as a signal to monitor the binding of rCdRP. The results obtained with IGPS[1−259] are shown in Figure 4. The isoemissive point at 393 nm indicates that only a single binding mode of rCdRP is involved. The K_d values are summarized in Table 6, which also includes the K_d and K_i values of yeast PRAI (xPRAI; Hommel et al., 1995). The K_d values generally agree well with competitive inhibition by rCdRP (K_i, Table 5).

Unfortunately, fluorescence titration of IGPS[1−252FAG] with rCdRP gave no reliable results. The signal was weak as a consequence of the practical upper limit of protein concentration (0.5 μM) before the onset of aggregation. Moreover, in contrast to PRAI[ML256−452] and IGPS[1−259], no saturation of the enzyme at high concentrations of rCdRP was observed. This complication might be due to some unspecific, perhaps hydrophobic interaction of rCdRP with the protein.

Kinetics of Ligand Binding. The unique and sensitive fluorescence signals described earlier, as well as the monofunctional nature of both IGPS[1−259] and PRAI[ML256−452], allow a thorough examination of the kinetics of ligand binding. The transients obtained for IGPS[1−259] from both fluorescence energy transfer and fluorescence quenching measurements were monoexponential (e.g., Figure 5A) and exhibited a similar dependence on the concentration of rCdRP (Figure 5B). Similar behavior was observed with PRAI[ML256−452] (Hommel et al., 1995). The kinetics of ligand binding was evaluated on the basis of the simplest possible model:

$$\text{P} + \text{L} \underset{k_D}{\overset{k_R}{\rightleftharpoons}} \text{PL} \qquad (2)$$

Under the conditions of small deviations of the initial reactant concentrations from the equilibrium values, the observed relaxation rate constant (Bernasconi, 1976) is given by

$$k_{obs} = k_D + k_R([\bar{\text{L}}] + [\bar{\text{P}}]) \qquad (3)$$

where $[\bar{\text{L}}]$ and $[\bar{\text{P}}]$ are the equilibrium concentrations of the ligand and the binding site, respectively. These were calculated from $[\text{L}]_o$ and $[\text{P}]_o$ according to eq 1, using the relationship $K_d = k_D/k_R$. Values of k_D and k_R, the dissociation and recombination rate constants, respectively, were calculated iteratively from eqs 3 and 1 by a least-squares method using a program described elsewhere (Eberhard, 1990b), and Table 7 summarizes the results.

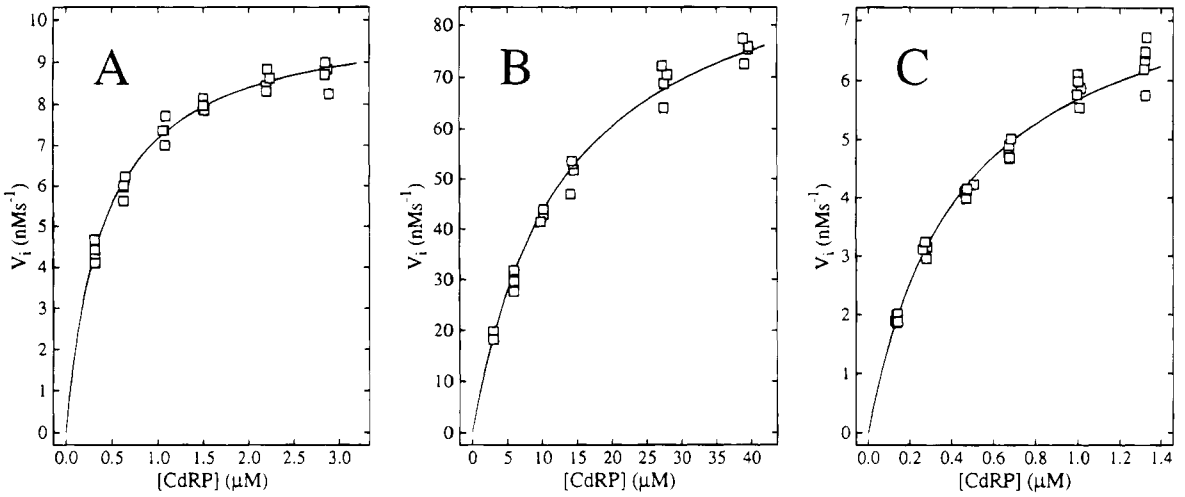

FIGURE 1: Comparison of the catalytic efficiencies of monofunctional IGPS domains with that of the bifunctional enzyme: analysis of initial velocities of the IGPS reaction. (A) IGPS:PRAI, four repetitive experiments in buffer C at 25 °C. The concentration of enzyme was 3.35 nM. k_{cat} = 3.24 s^{-1}, K_M = 0.42 μM. The steady state parameters are not significantly different when determined in buffer B (Eberhard, 1990a). (B) IGPS[1−252FAG], four repetitive experiments in buffer B at 25 °C. The concentration of IGPS[1−252FAG] was 23 nM. k_{cat} = 4.3 s^{-1}, K_M = 12.9 μM. 100 μL of a prewarmed (25 °C) solution of IGPS[1−252FAG] (230 nM) in buffer B was added to 900 μL of buffer B containing CdRP to start the reaction. (C) IGPS[1−259], same conditions as in (A), five repetitive experiments. The concentration of IGPS[1−259] was 3.42 nM. k_{cat} = 2.4 s^{-1}, K_M = 0.46 μM.

The calculated thermodynamic equilibrium constants (k_D/k_R) agree reasonably well with those obtained from equilibrium measurements (Table 6). However, the rate constants of rCdRP binding to the IGPS domain of IGPS:PRAI are substantially higher than those of IGPS[1−259]. The value of k_D for IGPS[1−259] is subjected to a considerable error, since it is obtained by extrapolation. The rate constants of PRAI[ML256−452] are about 2-fold higher than those of the bifunctional enzyme.

DISCUSSION

The properties of IGPS[1−259] demonstrate that the catalytic efficiency and structural integrity of IGPS are intrinsic properties; they do not depend significantly on its fusion with the PRAI domain. The crystal structure of IGPS-[1−259], which does not reveal substantial structural changes compared with the bifunctional enzyme (Wilmanns et al., 1990, 1992), supports this conclusion. The PRAI domain exhibits practically the same catalytic and ligand binding properties whether fused to the IGPS domain or as monofunctional enzyme, indicating that the PRAI domain is also a stable, autonomous entity.

The k_{cat}/K_M value of IGPS[1−252FAG] is about 20-fold smaller than that of IGPS[1−259] due to a 20-fold increase in the K_M value (Table 5). The changes in sequence compared to the bifunctional enzyme (Leu 253 to Phe and Leu 254 to Ala in the case of IGPS[1−252FAG], additional residues Glu-Asn-Lys-Val at the C-terminus in the case of IGPS[1−259]; cf. Scheme 1) are readily accommodated in the structure of the IGPS domain in IGPS:PRAI. Moreover, the carboxyl-terminally attached four residues of IGPS[1−259] appear to be mobile in the crystal structure (Wilmanns et al., 1990). There is no *a priori* obvious reason for the differences in solubility and kinetic properties between IGPS-[1−259] and IGPS[1−252FAG], apart from the presence of two additional charged residues in the carboxyl-terminal extension of the former. Since IGPS[1−252FAG] remains prone to aggregation even after isolation in pure monomeric form using HPLC gel filtration (not shown), it is conceivable that IGPS[1−252FAG] exists under native conditions as an equilibrium between the native, fully active (P) and a partially folded structure (I):

$$PL \rightleftharpoons P + L \rightleftharpoons I + L$$

If only P were able to bind the substrate (L), the coupling of an unfavorable equilibrium to the binding step would decrease the affinity of the enzyme for CdRP and thus lead to the observed increase in the K_M value, leaving k_{cat} unchanged (Table 5). This mechanism would also explain the different solubilities of IGPS[1−259] and IGPS[1−252FAG], assuming that I tends to aggregate:

$$nI \rightarrow \rightarrow (I)_n$$

From the crystal structure of IGPS:PRAI (Wilmanns et al., 1992), and from a comparison of the sequences of IGPS and PRAI from various organisms, it is likely that the bifunctional enzyme found in *E. coli* has arisen by gene fusion. The DNA sequence of the tryptophan operon of *E. coli* (Horowitz et al., 1983) reveals that the linker segments between the genes are either very short or absent (Das & Yanofsky, 1984). Only a few substitutions and deletions of an intercistronic nucleotide sequence are required to remove the stop codon of the upstream gene and to bring the downstream gene into the correct reading frame. The failure to demonstrate that IGPS[1−259] and PRAI[ML256−452] can form a noncovalent complex shows that the covalent linkage at Gly 255 is essential for stabilizing the defined interaction between the domains in the native bifunctional enzyme.

It is interesting what the selective advantage of gene fusion might have been, in the case of IGPS and PRAI, to the ancestor of *E. coli*. However, the active sites of IGPS and PRAI are neither connected by a tunnel, as in the case of tryptophan synthase (Hyde et al., 1988), nor do the two active sites interact during the binding of rCdRP (Cohn et al., 1979). The experiments of Cohn et al. (1979) also argue against the possibility of surface channeling, an interesting variant

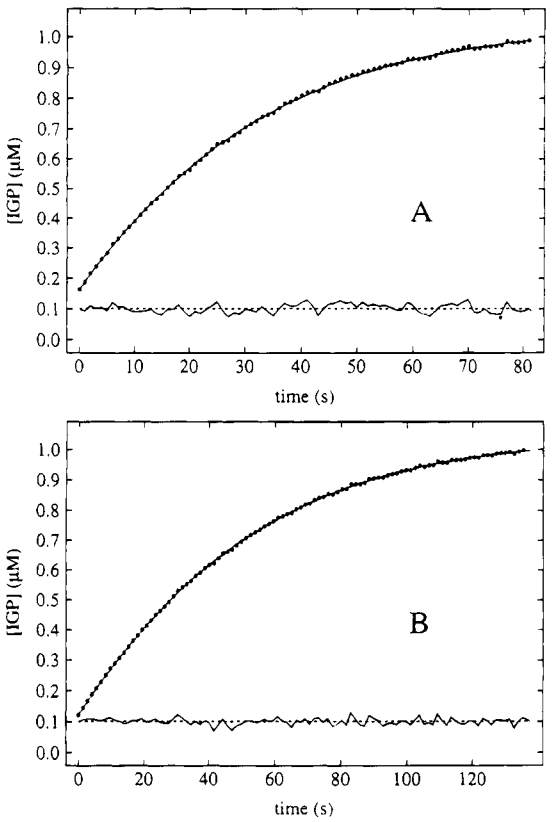

FIGURE 2: Comparison of the catalytic efficiencies of monofunctional IGPS[1−259] with that of the bifunctional enzyme: progress curve analysis of the IGPS reaction. The signal was normalized to the initial and final levels of fluorescence (excited at 280 nm, observed at 350 nm). The contribution of protein fluorescence to the initial signal was determined separately and subtracted from the transient. Conditions: 1.2 μM CdRP in buffer C at 25 °C. The dots represent the measured signal, and the solid curve represents a least-squares fit to the integrated Michaelis−Menten equation, which accounts for product inhibition. The bottom curve represents the residuals, i.e., the deviation of the experimental values from the theoretical curve (4-fold enlarged). (A) IGPS:PRAI (final concentration 12 nM). K_M = 0.32 μM, K_P = 0.51 μM, k_{cat} = 3.2 s^{-1}. The transient begins at [IGP] = 164 nM. (B) IGPS[1−259] (final concentration 10 nM). Same conditions as in (A). K_M = 0.44 μM, K_P = 0.86 μM, k_{cat} = 2.5 s^{-1}. The transient begins at [IGP] = 121 nM.

of interaction between active sites of bifunctional enzymes (Knighton et al., 1994). A significant increase in enzymatic activity upon gene fusion could provide a sufficiently selective advantage to an organism possessing a bifunctional enzyme. Since the catalytic efficiencies (k_{cat}/K_M) of the separate proteins are practically identical to those of the domains of the bifunctional enzyme, our results reinforce the previous conclusion (Kirschner et al., 1980) that the stabilization of the intrinsically labile IGPS domain by interdomain interactions is functionally advantageous.

Kinetic analysis of tryptophan biosynthetic enzymes from *E. coli* and yeast (Hommel et al., 1995) has shown that the specific activity of PRAI is about 10-fold higher than that of IGPS, tryptophan synthase (Lane & Kirschner, 1991), and PRT (Hommel et al., 1989). In several organisms, expression of PRAI seems to be less strictly regulated than that in the remaining enzymes (Crawford, 1989), leading to an excess of PRAI activity in the cell. This strategy keeps the intracellular steady state concentration of PRA low, because PRA is both expensive in terms of the metabolic energy required for its synthesis and chemically very unstable

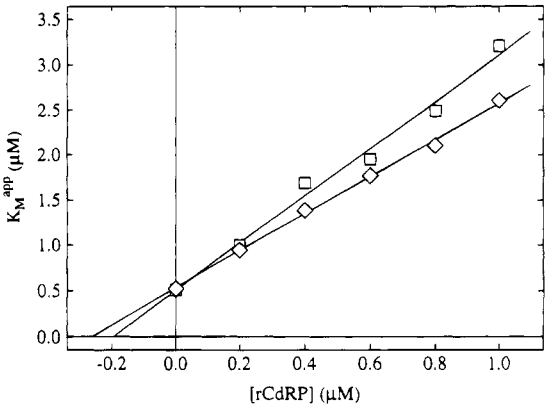

FIGURE 3: Competitive inhibition of IGPS by rCdRP: (□) IGPS:PRAI; (◇) IGPS[1−259]. Each point was determined from six individual saturation curves (v_i versus [CdRP], cf. Figure 1). The solid lines represent linear least-squares fits to the experimental data. The intersection with the vertical axis indicates the K_M value (0.51 μM for IGPS:PRAI, 0.54 μM for IGPS[1−259]), and the intersection with the horizontal axis indicates the negative value of K_i (0.19 μM for IGPS:PRAI, 0.26 μM for IGPS[1−259]).

Table 5: Steady State Kinetic Constants of IGPS and PRAI in Buffer C[a]

reaction	enzyme	k_{cat} (s^{-1})	K_M (μM)	k_{cat}/K_M (μM^{-1} s^{-1})	K_P[b] (μM)	K_i[c] (μM)
IGPS	IGPS:PRAI	3.6	0.42	8.6	0.54	0.19
	IGPS:PRAI[d]	4.0	0.51	7.8	nd[e]	nd
	IGPS[1−252FAG][d]	4.3	13	0.33	nd	nd
	IGPS[1−259]	3.2	0.47	6.8	0.81	0.26
PRAI	IGPS:PRAI	40	4.9	8.2	nd	6.5[f]
	PRAI[ML256−452]	32	4.7	6.8	6.2	6.8[f]

[a] Average values from initial velocity and progress curve measurements as exemplified in Figures 1 and 2. [b] Product inhibition by CdRP. [c] Competitive inhibition by rCdRP. [d] Buffer B. [e] nd: not determined. [f] From Hommel et al. (1995).

(Creighton, 1968). Moreover, tryptophan biosynthesis involves a spontaneous (and under physiological conditions perhaps even rate-limiting) isomerization of one of its intermediates (CdRP; Hommel et al., 1995). Apparently, there is no requirement to match the activities of PRAI and IGPS *in vivo*.

Inspection of the crystal structure of IGPS:PRAI reveals a domain−domain interaction consisting of eight putative hydrogen bonds and numerous hydrophobic contacts (Wilmanns et al., 1992). Nevertheless, the noncovalent interaction between the isolated domains is so weak as to be indiscernible. This observation may be due to structural changes at the domain−domain interface incurred by the separation (cf. Scheme 1 for changes in sequence). The only evidence for a functionally important interaction between IGPS and PRAI comes from studies of the multifunctional enzyme from *Neurospora crassa* containing both PRAI and IGPS activity (Gaertner et al., 1970).

The binding of rCdRP to both IGPS[1−259] and PRAI[ML256−452] occurs in a single step. In contrast to IGPS:PRAI (Cohn et al., 1979), no isomerization process follows the initial binding to the active site of IGPS. Tryptophan 356, which is located at the bottom of the active site of the PRAI domain in the vicinity of the domain−domain interface (Wilmanns et al., 1992), may possibly respond differently to structural changes upon ligand binding, depending on whether it is connected to the IGPS domain. Moreover, the

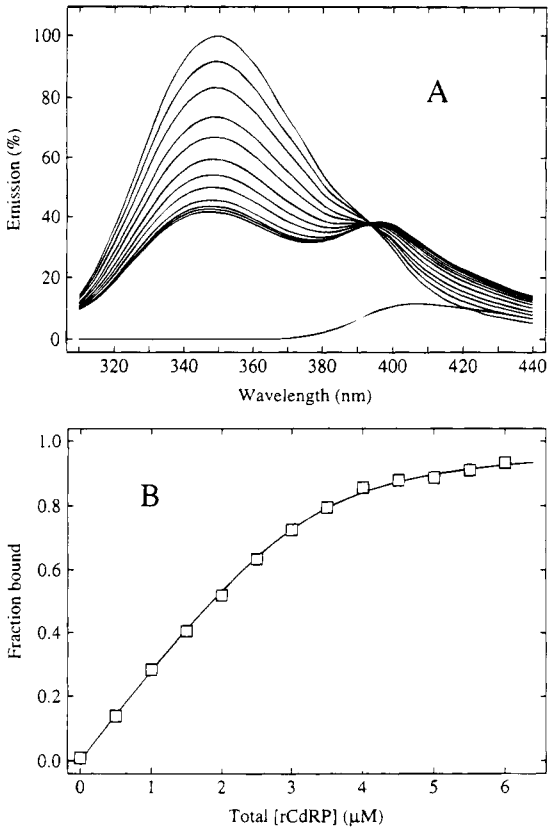

FIGURE 4: IGPS[1−259] has a single high-affinity binding site for rCdRP. Fluorescence was excited at 280 nm. (A) Fluorescence emission spectra of IGPS[1−259] (3.24 μM, in buffer C at 25 °C) titrated with rCdRP in increments of 0.5 μM. The fluorescence intensity decreased at 350 nm and increased at 400 nm upon the addition of rCdRP. The spectrum with the highest peak at 350 nm is that of unliganded IGPS[1−259], and the bottom spectrum is that of 10 μM rCdRP. (B) Binding curve of rCdRP to IGPS[1−259]. Evaluation of fluorescence quenching at 350 nm, where rCdRP does not contribute to the signal. The solid curve is the least-squares fit to eq 1 (cf. Experimental Procedures) with K_d = 0.26 μM and n = 0.81.

Table 6: Thermodynamic Dissociation Constants and Competitive Inhibition Constants of rCdRP Bound to IGPS and PRAI

protein	K_d (μM)	K_i (μM)	reference figures
IGPS:PRAI[a]	0.22[b]	0.19,[c] 0.3[b]	3
IGPS[1−259]	0.26	0.26[c]	4, 3
IGPS:PRAI[d]	12.5[b]	6.9[c]	
PRAI[ML256−452]	7.8[e]	6.8[c]	
xPRAI	1.8[e]	2.2[e]	

[a] Binding to the active site of the IGPS domain. [b] Value obtained by Bisswanger et al. (1979) in 0.1 M Tris-acetate (pH 7.5) at 20 °C. [c] Data from Table 5. [d] Binding to the active site of the PRAI domain. [e] Hommel et al. (1995).

experiments of Cohn et al. (1979) were performed in 0.1 M Tris−acetate buffer at pH 7.5, whereas the present studies were carried out in 0.05 M Tris-HCl buffer at pH 7.5 in the presence of 4 mM Mg^{2+}. Table 7 reveals differences between the rate constants of rCdRP binding to IGPS. In particular, k_D^{rCdRP} is 10-fold smaller for IGPS[1−259] than for IGPS:PRAI. These differences could be due to altered flexibility of the loops involved in the binding of the ligand.

As a consequence of the rather similar catalytic and ligand binding properties between IGPS:PRAI and both PRAI[ML256−452] and IGPS[1−259], the isolated domains appear to be good models for the corresponding domains of

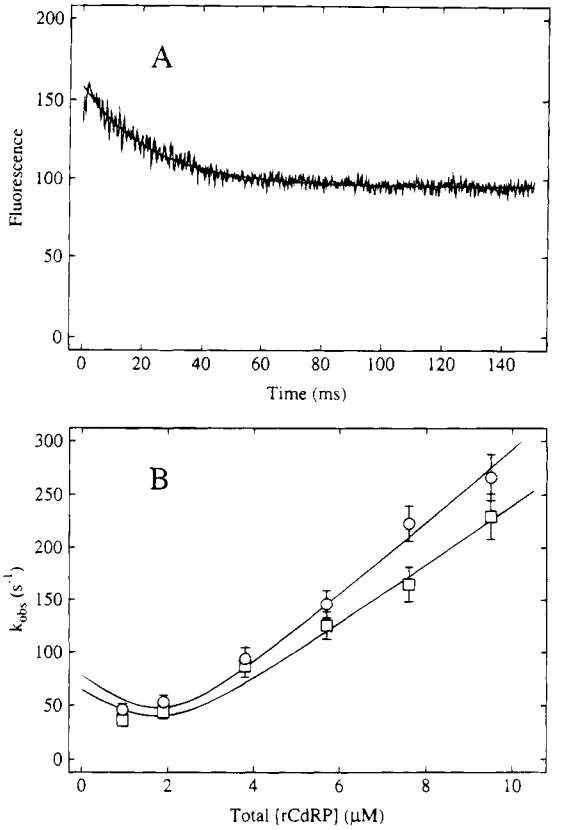

FIGURE 5: Kinetics of rCdRP binding to IGPS[1−259]. Stopped-flow measurements were performed in buffer C at 25 °C. Values refer to initial concentrations after mixing. (A) Single stopped-flow transient observed after the mixing of IGPS[1−259] (2.2 μM) with rCdRP (1.0 μM). Protein fluorescence was excited at 280 nm and observed using a bandpass filter (330−380 nm). The solid curve is the best fit exponential decay calculated by least-squares methods (k_{obs} = 43.5 s^{-1}). (B) Dependence of k_{obs} on [rCdRP]. The concentration of IGPS[1−259] was 2.2 μM for each point. (□) Fluorescence quenching (cf. Figure 4A, k_R= 35 μM^{-1} s^{-1}, k_D= 8.1 s^{-1}). (○) Fluorescence energy transfer (k_R = 29 μM^{-1} s^{-1}, k_D = 7.0 s^{-1}). Each point represents the rate constant evaluated from the average of 10−15 transients. The solid curves and determinations of k_D and k_R values by least-squares fits to eq 3 (Experimental Procedures).

Table 7: Kinetics of rCdRP Binding to IGPS and PRAI[a]

protein	k_R (μM^{-1} s^{-1})	k_D (s^{-1})	k_D/k_R (μM)
IGPS:PRAI[b]	100	80	0.8
IGPS[1−259]	32	8	0.25
IGPS:PRAI[c]	14	140	10
PRAI[ML256−452]	23	280	12

[a] Average values of rate constants determined by fluorescence energy transfer and fluorescence quenching (cf. Figure 5B). [b] Active site of IGPS, evaluation of the more rapid of the two exponential progress phases (Cohn et al., 1979). [c] Active site of PRAI, where a single binding phase was observed (Cohn et al., 1979).

the bifunctional enzyme. For example, the binding of CdRP to the active site of PRAI cannot be analyzed conveniently with the bifunctional enzyme. Moreover, comparison of the two monofunctional enzymes from *E. coli* (PRAI[ML256−452]) and yeast (xPRAI) provides interesting insights into the divergent evolution of this enzyme (Hommel et al., 1995).

ACKNOWLEDGMENT

We thank Paul Zenö for amino acid analyses and Ariel Lurtig for performing the ultracentrifugation runs. Halina

Szadhowsky was of great help in purifying the separated domains.

REFERENCES

Bernasconi, C. F. (1976) in *Relaxation Kinetics*, Academic Press, New York.

Bisswanger, H., Kirschner, K., Cohn, W., Hager, V., & Hansson, E. (1979) *Biochemistry 18*, 5946−5953.

Bradford, M. M. (1976) *Anal. Biochem. 72*, 248−254.

Braus, G. H., Luger, K., Paravicini, G., Schmidheini, T., Kirschner, K., & Hütter, R. (1988) *J. Biol. Chem. 263*, 7868−7875.

Brzovic, P. S., Ngo, K., & Dunn, M. F. (1992) *Biochemistry 31*, 3831−3839.

Cohn, W., Kirschner, K., & Paul, C. (1979) *Biochemistry 18*, 5953−5959.

Cornish-Bowden, A. (1975) *Biochem. J. 149*, 305−312.

Crawford, I. P. (1989) *Annu. Rev. Microbiol. 43*, 567−600.

Creighton, T. E. (1968) *J. Biol. Chem. 243*, 5605−5609.

Creighton, T. E. (1970) *Biochem. J. 120*, 699−707.

Das, A., & Yanofsky, C. (1984) *Nucleic Acids Res. 12*, 4757−4768.

Duggleby, R. G., & Morrison, J. F. (1977) *Biochim. Biophys. Acta 481*, 297−312.

Eberhard, M. (1990a) Ph.D. Thesis, University of Basel, Basel, Switzerland.

Eberhard, M. (1990b) *CABIOS 6*, 213−221.

Gaertner, F. H., Ericson, M. C., & DeMoss, J. A. (1970) *J. Biol. Chem. 245*, 595−600.

Hommel, U. (1988) Ph.D. Thesis, University of Basel, Basel, Switzerland.

Hommel, U., Lustig, A., & Kirschner, K. (1989) *Eur. J. Biochem. 180*, 33−40.

Hommel, U., Eberhard, M., & Kirschner, K. (1995) *Biochemistry 34*, 5429−5439.

Horowitz, H., Van Arsdell, J., & Platt, T. (1983) *J. Mol. Biol. 169*, 775−797.

Hum, D. W., & MacKenzie, R. E. (1991) *Protein Eng. 4*, 493−500.

Hütter, R., Niederberger, P., & DeMoss, J. A. (1986) *Annu. Rev. Microbiol. 40*, 55−77.

Hyde, C. C., Ahmed, S. A., Padlan, E. A., Miles, E. W., & Davis, D. R. (1988) *J. Biol. Chem. 263*, 17857−17871.

Kirschner, K., Szadkowski, H., Henschen, A., & Lottspeich, F. (1980) *J. Mol. Biol. 143*, 395−409.

Kirschner, K., Szadkowski, H., Jardetzky, T. S., & Hager, V. (1987) *Methods Enzymol. 142*, 386−397.

Kirschner, K., Lane, A. N., & Strasser, A. W. (1991) *Biochemistry 30*, 472−478.

Knecht, R., & Chang, J.-Y. (1986) *Anal. Chem. 58*, 2375−2379.

Knighton, D. R., Kan, C.-C., Howland, E., Janson, C. A., Hostomska, Z., Welsh, K. M., & Matthews, D. A. (1994) *Nature Struct. Biol. 1*, 186−194.

Kramer, W., Drutsa, V., Jansen, H.-W., Kramer, B., Plugfelder, M., & Fritz, H.-J. (1984) *Nucleic Acids Res. 12*, 9441−9456.

Lane, A. N., & Kirschner, K. (1991) *Biochemistry 30*, 479−484.

Levine, L. L., & Federici, M. M. (1982) *Biochemistry 21*, 2600−2606.

Luger, K., Hommel, U., Herold, M., Hofsteenge, J., & Kirschner, K. (1989) *Science 243*, 206−210.

Maniatis, T., Fritsch, E. F., & Sambrook, J. (1982) *Molecular Cloning*, Cold Spring Harbor Laboratory Press, Cold Spring Harbor, NY.

Marquardt, D. W. (1963) *J. Soc. Ind. Appl. Math. 11*, 431−441.

Messing, J., & Vieira, J. (1982) *Gene 19*, 269−276.

Paul, C., Kirschner, K., & Haenisch, G. (1980) *Anal. Biochem. 101*, 442−448.

Pflugfelder, M. (1986) Ph.D. Thesis, University of Basel, Basel, Switzerland.

Priestle, J. P., Grütter, M. G., White, J. L., Vincent, M. G., Kania, M., Wilson, E., Jardetzky, T. S., Kirschner, K., & Jansonius, J. N. (1987) *Proc. Natl. Acad. Sci. U.S.A. 84*, 5690−5694.

Sanger, F., Nicklen, S., & Coulson, A. R. (1977) *Proc. Natl. Acad. Sci. U.S.A. 74*, 5463−5467.

Schneider, W. P., Nichols, B. P., & Yanofsky, C. (1981) *Proc. Natl. Acad. Sci. U.S.A. 78*, 2169−2173.

Shine, J., & Dalgarno, L. (1974) *Proc. Natl. Acad. Sci. U.S.A. 71*, 1342−1346.

Stanssens, P., Opsomer, C., McKeown, Y. M., Kramer, W., Zabeau, M., & Fritz, H.-J. (1989) *Nucleic Acids Res. 17*, 4441−4454.

Stewart, J., Wilson, D. B., & Ganem, B. (1990) *J. Am. Chem. Soc. 112*, 4582−4584.

Tandon, S., & Horowitz, P. M. (1988) *J. Biol. Chem. 264*, 9859−9866.

Vieira, J., & Messing, J. (1982) *Gene 19*, 259−268.

Washabaugh, M. W., & Collins, K. D. (1986) *J. Biol. Chem. 261*, 12477−12485.

Wilmanns, M., Schlagenhauf, E., Fol, B., & Jansonius, J. N. (1990) *Protein Eng. 3*, 173−180.

Wilmanns, M., Priestle, J. P., Niermann, T., & Jansonius, J. N. (1992) *J. Mol. Biol. 223*, 477−507.

BI941804S